



ALICE

J/ ψ production in p-Pb with ALICE at the LHC



Outline

- Motivation
- Analysis
- Results
 - $d^2\sigma_{J/\psi}/dydp_T$
 - $d\sigma_{J/\psi}/dy$
 - $R_{FB}(\text{integrated})$
 - $R_{FB}(p_T)$
 - pp interpolation
 - $R_{pPb}(y_{cms})$ and $R_{Pbp}(y_{cms})$

In red are **final results** from :

J/ψ production and nuclear effects in p-Pb collisions at $\sqrt{s_{NN}}=5.02$ TeV
[arXiv:1308.6726](https://arxiv.org/abs/1308.6726)

Cold Nuclear Matter effects

[1] see e.g. Nucl. Phys. A700(2002)539

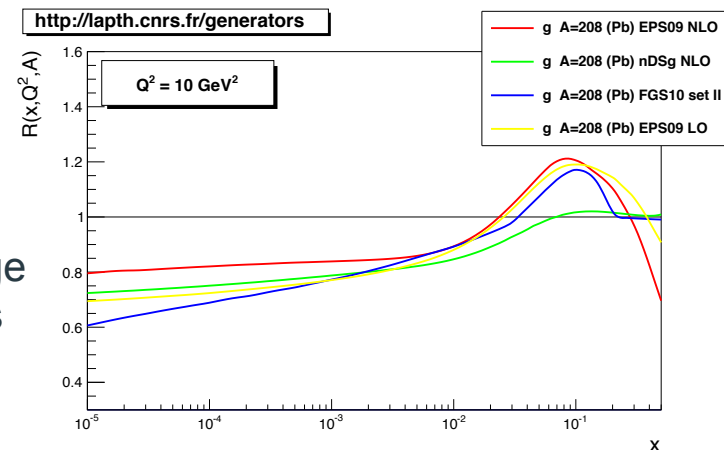
[2] see e.g. Phys.Rev.Lett. 109(2012)122301

[3] see e.g. JHEP0904(2009)065

- **nuclear absorption** [1]
 - expected to be small at LHC
 - as $c\bar{c}$ pairs spend a very short time within nuclear matter due to large Lorentz factor of the pair with respect to the nucleus

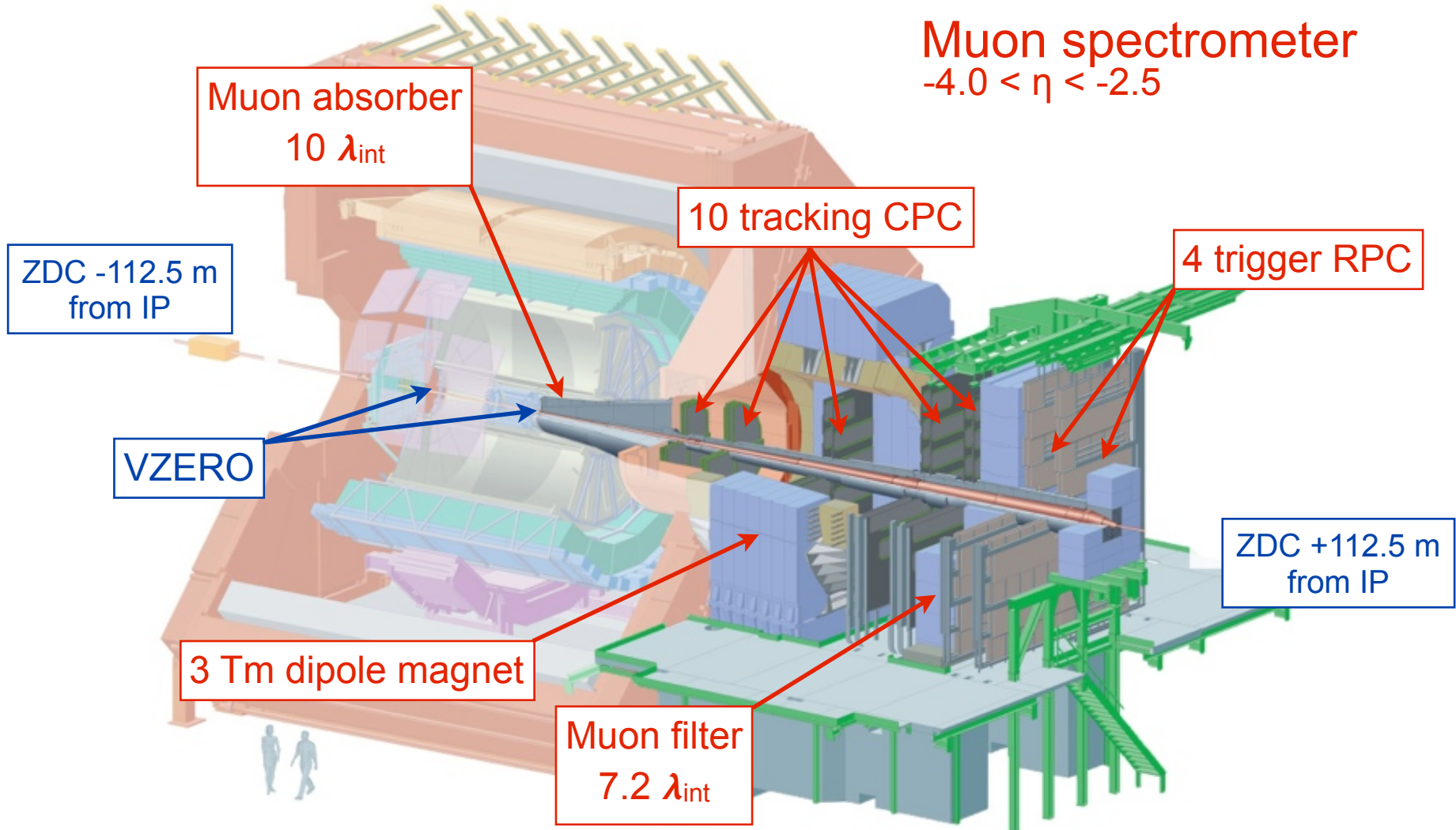
- **(coherent) energy loss** [2]
 - the amount of medium-induced gluon radiation impacts the strength of the J/psi suppression

- **initial state modification** [3]
 - **gluon shadowing** (or saturation)
 - shadowing expected to be large at LHC (but large uncertainties on nPDFs at low x)



Study of the CNM effects in p-Pb interesting in itself as well as for its consequences for Pb-Pb collisions

ALICE detector (for muons)



Data selection

EVENT SELECTION

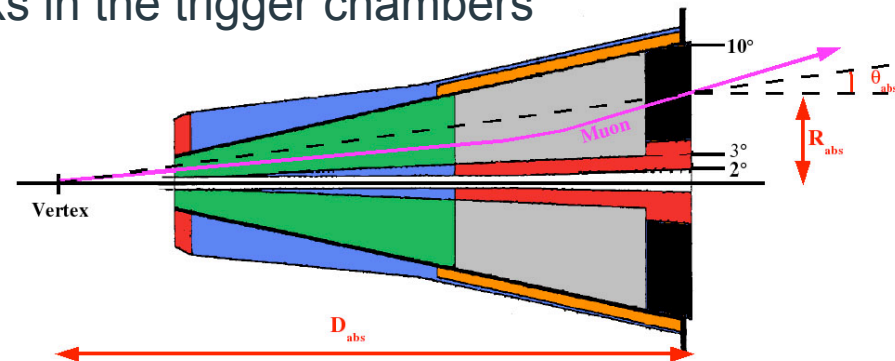
- Minimum Bias (MB) trigger : coincidence of the two sides of the VZERO ($2.8 < \eta < 5.1$ and $-3.7 < \eta < -1.7$)
- MB trigger efficiency $\sim 99\%$ for NSD events
- Rejection of beam-gas and electromagnetic interactions
- SPD used for vertex determination

DIMUON TRIGGER

- MB & two opposite sign muon tracks in the trigger chambers

ANALYSIS CUTS

- Muon trigger matching
- $-4.0 < \eta_\mu < -2.5$
- $17.6 \text{ cm} < R_{\text{abs}} < 89.5 \text{ cm}$ (where R_{abs} is the track radial position at the end of absorber)



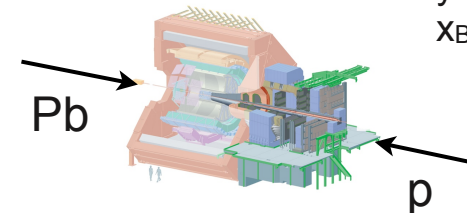
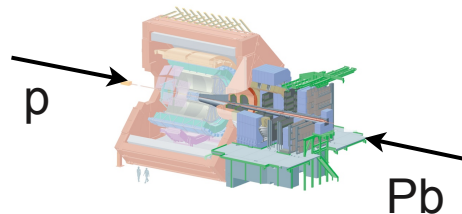
LHC beam energies asymmetry induces a **rapidity shift** of the NN-cms in the direction of the proton

$$\Delta y \approx \frac{1}{2} \log \frac{Z_{Pb} A_p}{Z_p A_{Pb}} = 0.465$$

Data executive summary

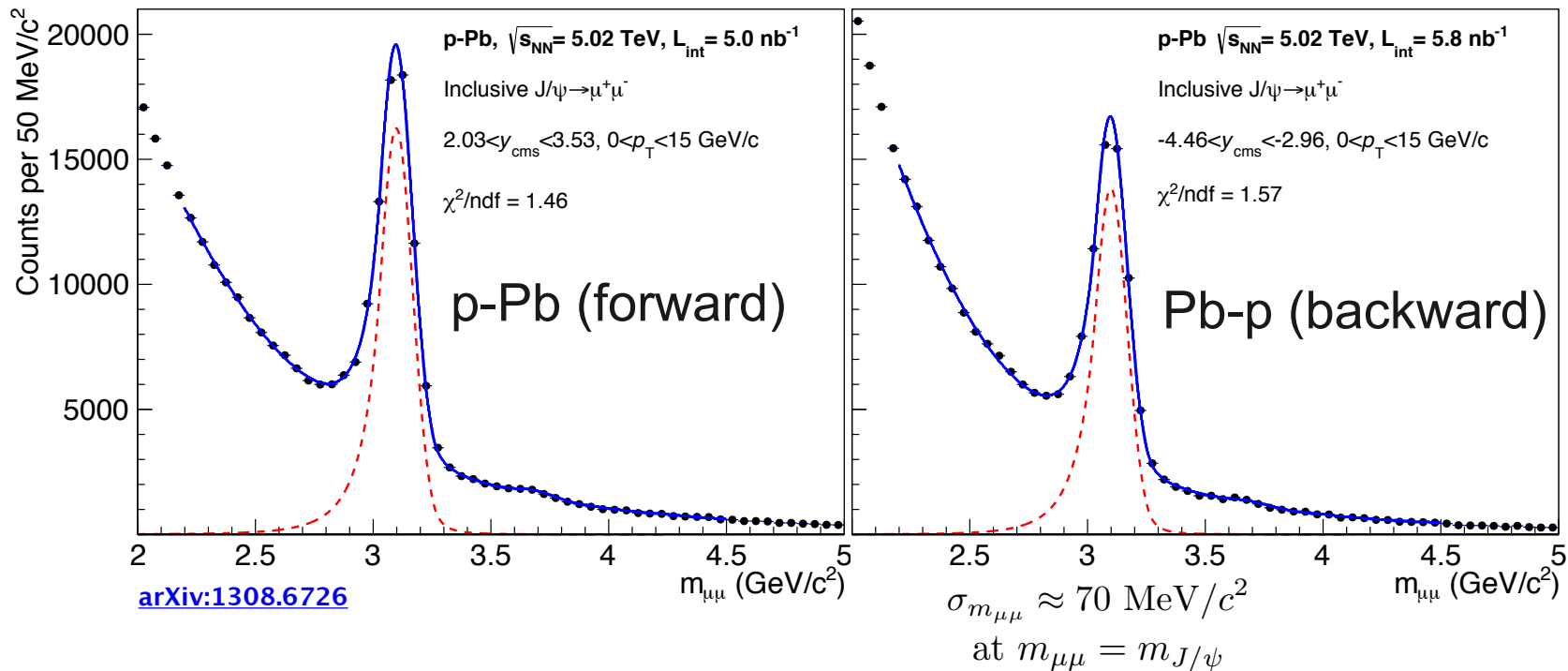
	p-Pb (forward)	Pb-p (backward)
$L_{\text{int}} \text{ (nb}^{-1}\text{)}$	5.03 ± 0.18	5.81 ± 0.19
$\sigma_{\text{MB}} \text{ (b)}$ (from VdM scans)	2.08 ± 0.07	2.12 ± 0.07
$N_{J/\psi} \text{ (} 10^4\text{)}$	$6.69 \pm 0.05 \pm 0.08$	$5.67 \pm 0.05 \pm 0.07$
$y_{\text{cms}} \text{ range}$	[2.03 ; 3.53]	[-4.46 ; -2.96]
$x_{\text{Bj}} \text{ range}$ (assuming 2->1 kinematics)	$1.8 - 8.1 \times 10^{-5}$	$1.2 - 5.3 \times 10^{-2}$

Note : PHENIX
@ 200 GeV
 $y=0$
 $x_{\text{Bj}}=1.5 \times 10^{-2}$



Signal extraction

Based on fits of the invariant mass of unlike-sign muon pairs

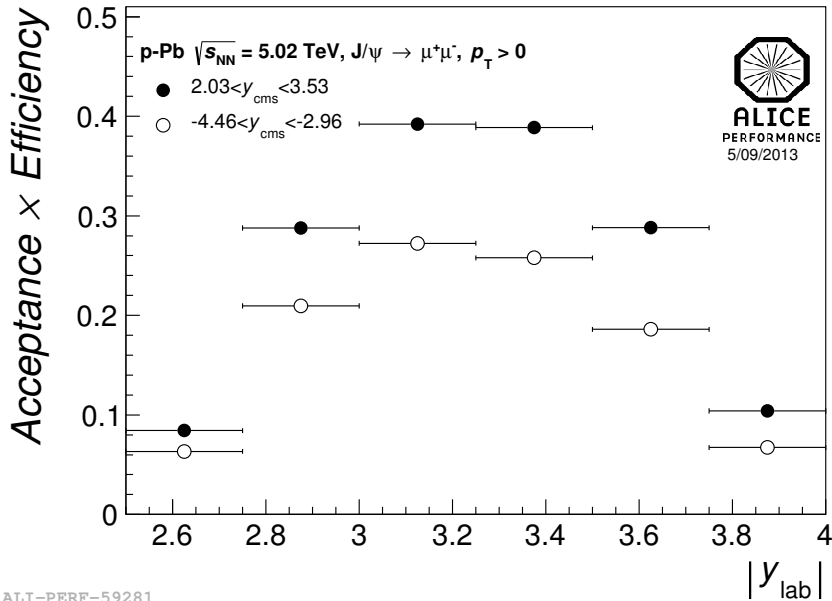


System. uncertainty computed varying :

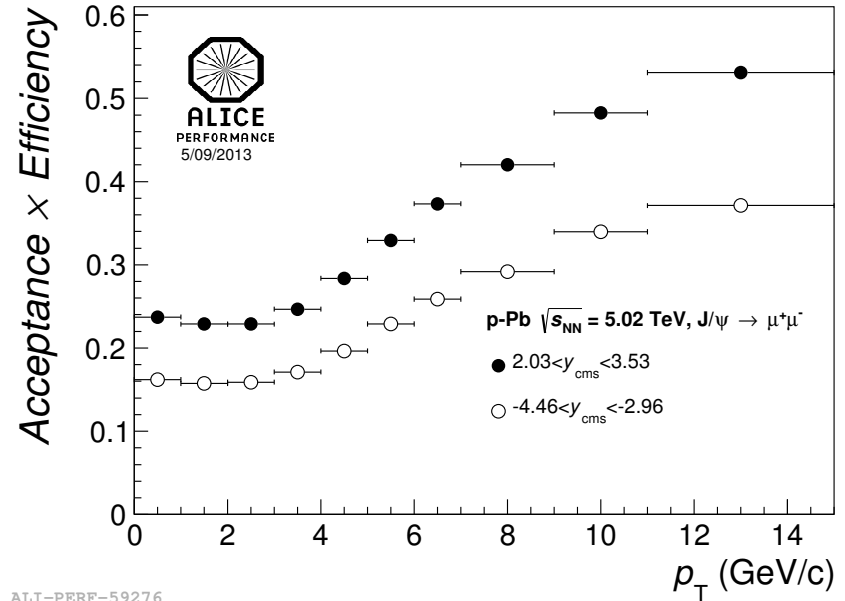
- **SIGNAL SHAPE** : extended Crystal Ball (CB2) or other pseudo-gaussian functions (tails tuned on the corresponding Monte Carlo (MC))
- **BACKGROUND SHAPE** : variable width gaussian (VWG) or polynomial x exponential
- **FITTING RANGE**

and amounts to **1-4%**

Acceptance x Efficiency



ALI-PERF-59281



ALI-PERF-59276

$$\langle Acc \times Eff \rangle_{pPb} = (25.4 \pm 1.3)\%$$

$$\langle Acc \times Eff \rangle_{Pbp} = (17.1 \pm 1.2)\%$$

Difference between p-Pb and Pb-p due to different efficiency of the detector in the two data-taking periods

Source of syst. unc.	<syst. unc.>
MC acceptance inputs	1.5%
tracking efficiency	4-6%
trigger efficiency	3 %
matching efficiency	1 %

Differential J/Ψ cross-section

$$\sigma_{J/\psi \rightarrow \mu^+ \mu^-} = \frac{N_{J/\psi \rightarrow \mu^+ \mu^-}}{L_{int} \times Acc \times Eff \times BR_{J/\psi \rightarrow \mu^+ \mu^-}}$$

$$L_{int} = \frac{N_{MB}}{\sigma_{MB}} \quad BR_{J/\psi \rightarrow \mu^+ \mu^-} = (5.93 \pm 0.06)\%$$

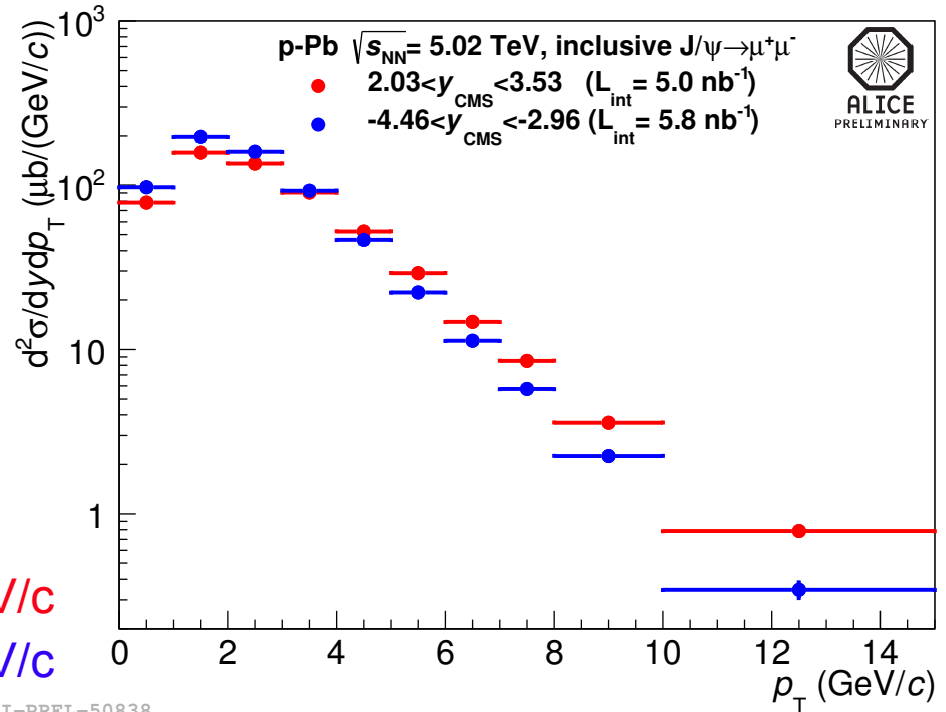
Source of syst. unc.	syst. unc.
signal extraction	1-4%
Acc x Eff	5-7%
L _{int}	3.5 %

$\langle p_T \rangle = 2.77 \pm 0.01(\text{stat.}) \pm 0.02(\text{syst.}) \text{ GeV}/c$

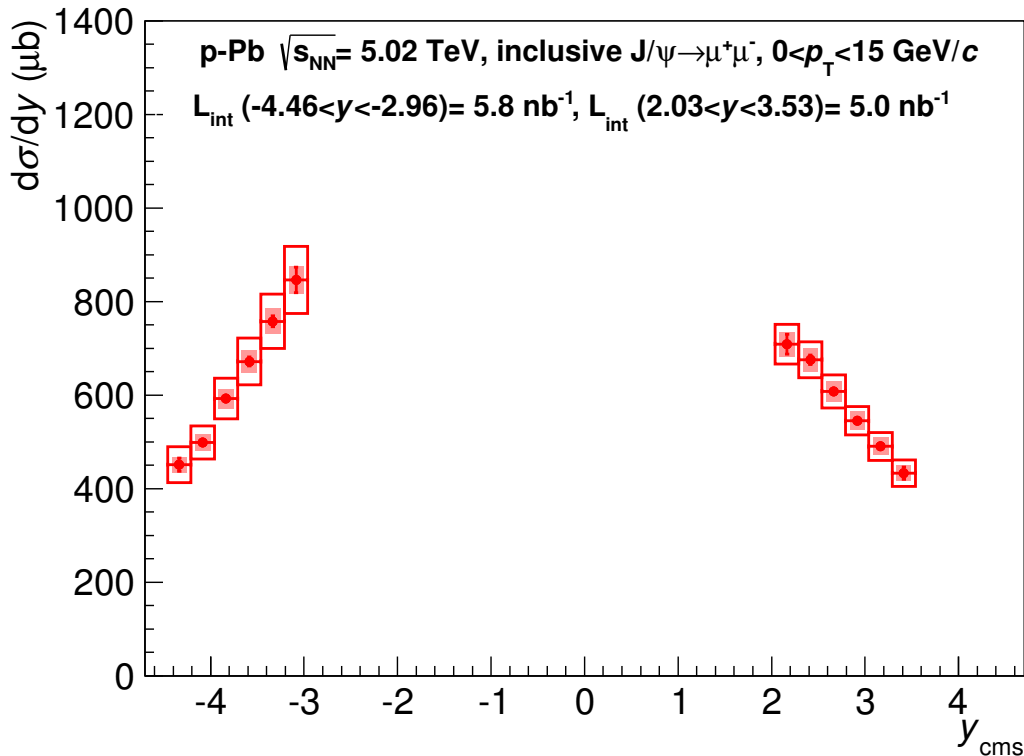
$\langle p_T \rangle = 2.47 \pm 0.01(\text{stat.}) \pm 0.02(\text{syst.}) \text{ GeV}/c$

ALI-PREL-50838

$\langle p_T \rangle$ is computed within $0 < p_T < 15 \text{ GeV}/c$



Cross-section vs rapidity



uncorrelated
uncertainties : matching,
 trigger eff, tracking eff, acc.
 inputs, signal extraction

(partially) correlated
uncertainties : luminosity,
 normalization factor, BR

statistical uncertainties

ALI-DER-59221

$$\frac{d\sigma_{Pbp}}{dy} = 644 \pm 5(\text{stat.}) \pm 51(\text{syst.})\mu\text{b}$$

$$\frac{d\sigma_{pPb}}{dy} = 588 \pm 4(\text{stat.}) \pm 38(\text{syst.})\mu\text{b}$$

Cross-sections are higher in the backward rapidity region (Pb-p)

Forward to Backward Ratio

$$\begin{aligned}
 R_{FB}^{J/\psi} &= \frac{Y_{J/\psi \rightarrow \mu^+ \mu^-}^{Forward}}{Y_{J/\psi \rightarrow \mu^+ \mu^-}^{Backward}} = \frac{R_{pPb}}{R_{Pbp}} \\
 &= \frac{N_{J/\psi \rightarrow \mu^+ \mu^-}^{Forward}}{N_{J/\psi \rightarrow \mu^+ \mu^-}^{Backward}} \times \frac{(Acc \times Eff)^{Backward}}{(Acc \times Eff)^{Forward}} \times \frac{N_{MB}^{Backward}}{N_{MB}^{Forward}}
 \end{aligned}$$

computed in the y_{cms} range common to both p-Pb and p-Pb

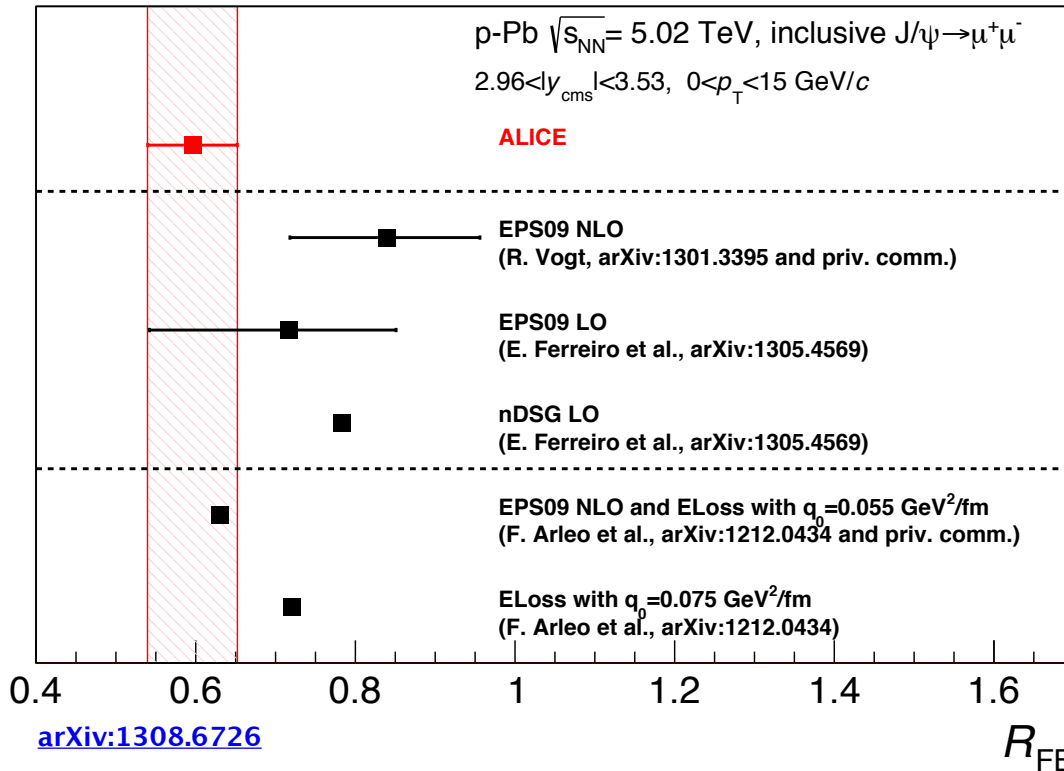
 loss of 2/3 of statistics

 no pp cross-section needed

	p-Pb	Pb-p
common y_{cms} range	[2.96 ; 3.53]	
y_{lab} range	[3.43 ; 4]	[-3.07 ; -2.5]
x_{Bj} range	1.8 - 3.2 x 10 ⁻⁵	1.2 - 2.1 x 10 ⁻²

Integrated R_{FB}

$$R_{FB} = 0.60 \pm 0.01(\text{stat.}) \pm 0.06(\text{syst.})$$



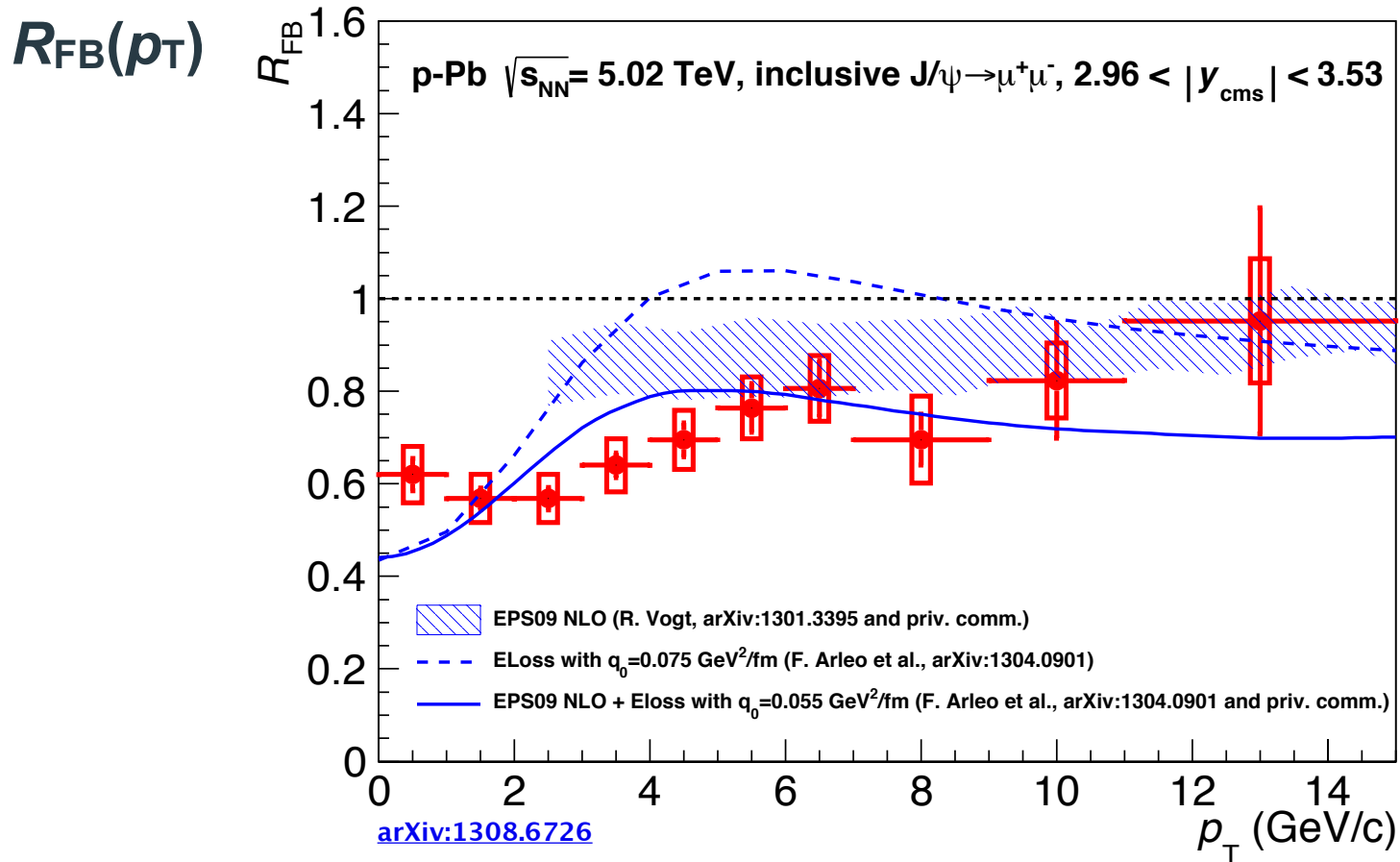
exp. uncertainty reasonably small

models w/ pure shadowing slightly overestimates the data

model including energy loss contribution shows good agreement with the data

(caveat: models over/undershooting the data can still get the R_{FB} right...)

R_{FB} y -dependence is flat, while p_T -dependence is not (next slide)



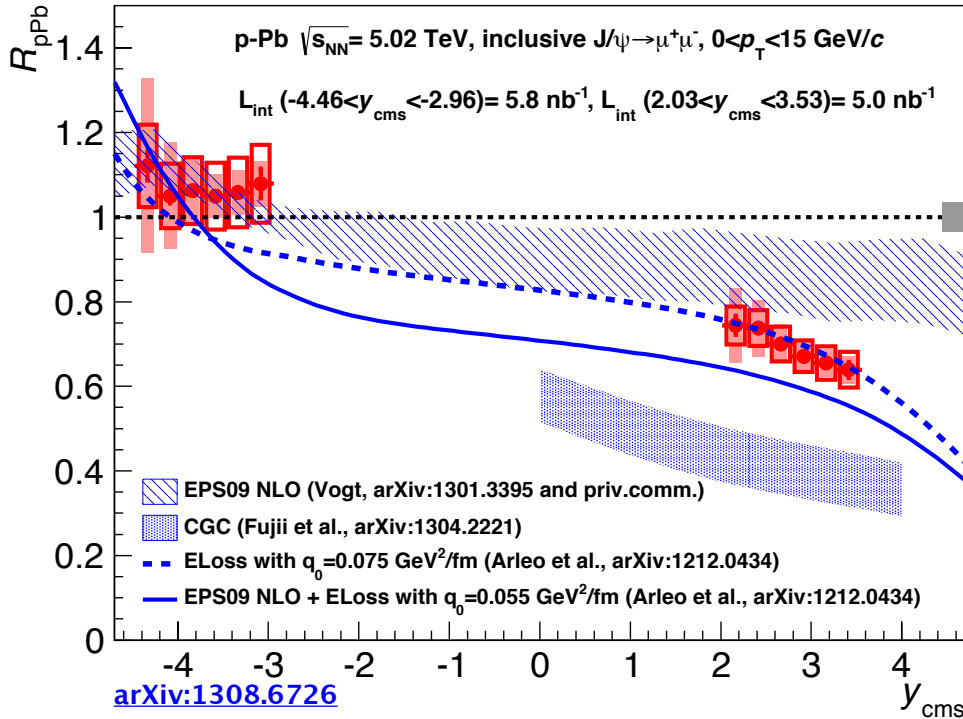
- stronger suppression at low p_T
 - fairly well reproduced by models including energy loss
- observed p_T -dependence is smoother than expected in coherent energy loss models

Further ingredients for R_{pPb} measurement

- Nuclear thickness function
 - $\langle T_{pPb} \rangle = 0.0983 \pm 0.0035 \text{ mb}^{-1}$ (from Glauber)
- pp reference : no measurement at the required energy, so need to **interpolate**
 - 2 steps procedure :
 - energy interpolation (for each y bin)
 - » using own available results for pp at 2.76 and 7 TeV ($2.5 < y_{\text{cms}} < 4.0$)
 - » 3 empirical shapes : linear, power law, exponential
 - rapidity extrapolation
 - » due to the $\Delta y=0.465$ shift, cannot directly use the above interpolations
 - » $d\sigma/dy$ fitted by various shapes (gaussian, polynomials) to reach the required y ranges
 - cross-checked with CEM and FONLL models

R_{pPb} and R_{PbPb} vs rapidity

$$R_{pPb} = \frac{N_{J/\psi \rightarrow \mu^+\mu^-}}{\sigma_{pp}^{J/\psi} \times \langle T_{pPb} \rangle \times N_{MB} \times Acc \times Eff \times BR_{J/\psi \rightarrow \mu^+\mu^-}}$$

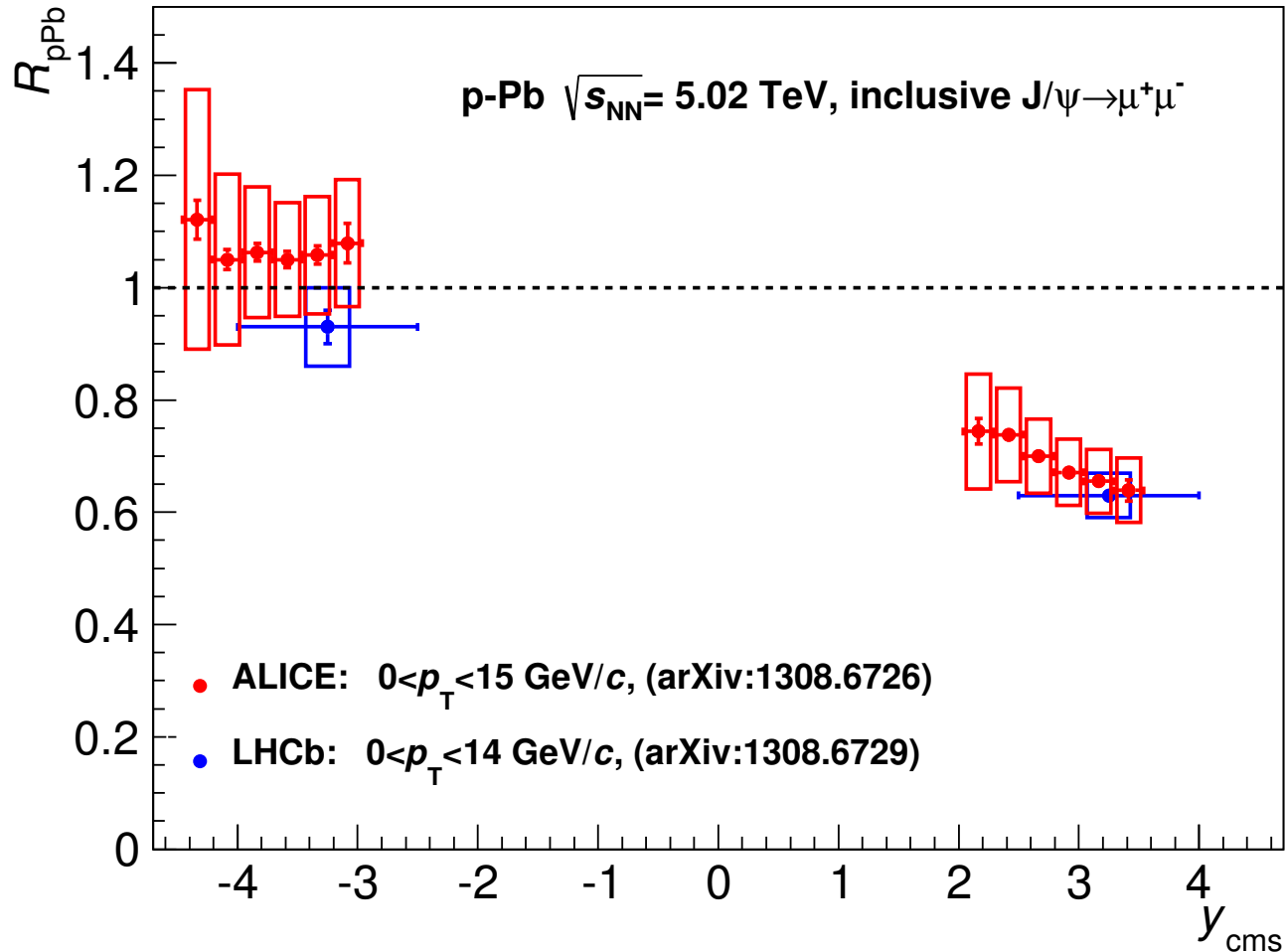


Source of syst. unc.	syst. unc.
Signal extraction	1-4%
Acc x Eff	5-7%
N_{MB}	1 %
$\langle T_{pPb} \rangle$	3.4%
σ_{pp}	5-18%

- Suppression at forward y
- No suppression at backward y

- At forward y data in between shadowing and energy loss models
- At backward y models including coherent parton energy loss show a slightly steeper pattern than the observed one
- Color Glass Condensate model (Fuji et al., forward y only) overestimates the suppression

ALICE vs LHCb : R_{pPb}



ALI-DER-59209

In this plot all systematic uncertainties are quadratically summed up

Conclusions

- R_{FB} shows a clear p_{T} dependence with a decrease at low p_{T}
 - in qualitative agreement with models including coherent energy loss contribution
- R_{pPb} show an increase of suppression towards forward rapidity
 - in agreement with energy loss model and/or shadowing model EPS09 NLO
- No suppression at backward rapidities



Thank you for your attention

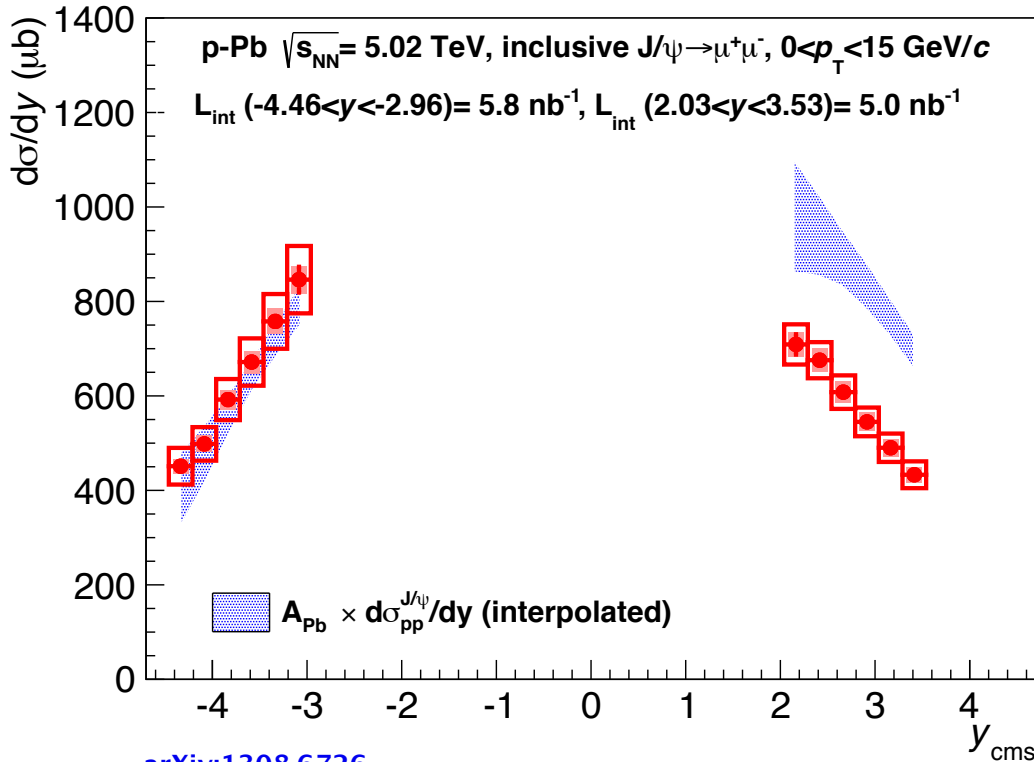
A Large Ion Collider Experiment



ALICE

BACKUPS

Cross-section vs rapidity in p-Pb vs pp interpolation



[arXiv:1308.6726](https://arxiv.org/abs/1308.6726)

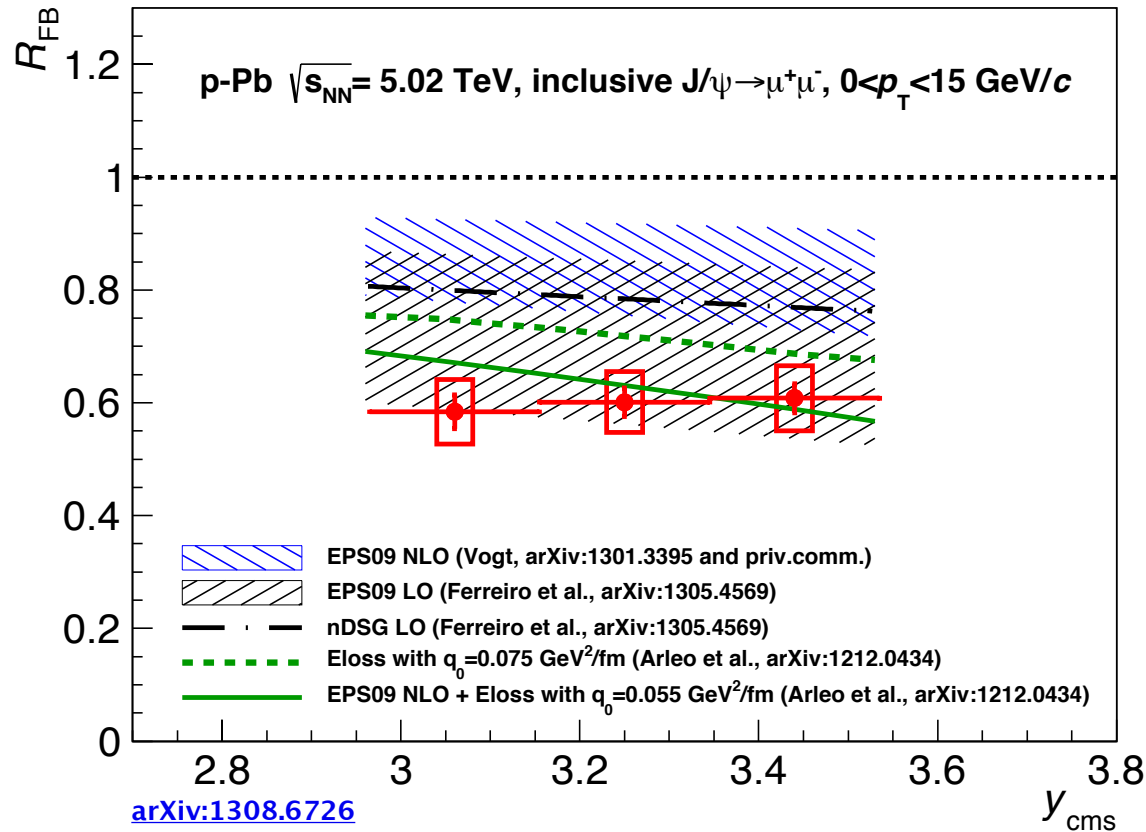
uncorrelated uncertainties : matching, trigger eff, tracking eff, acc. inputs, signal extraction

(partially) correlated uncertainties : luminosity, normalization factor, BR

statistical uncertainties

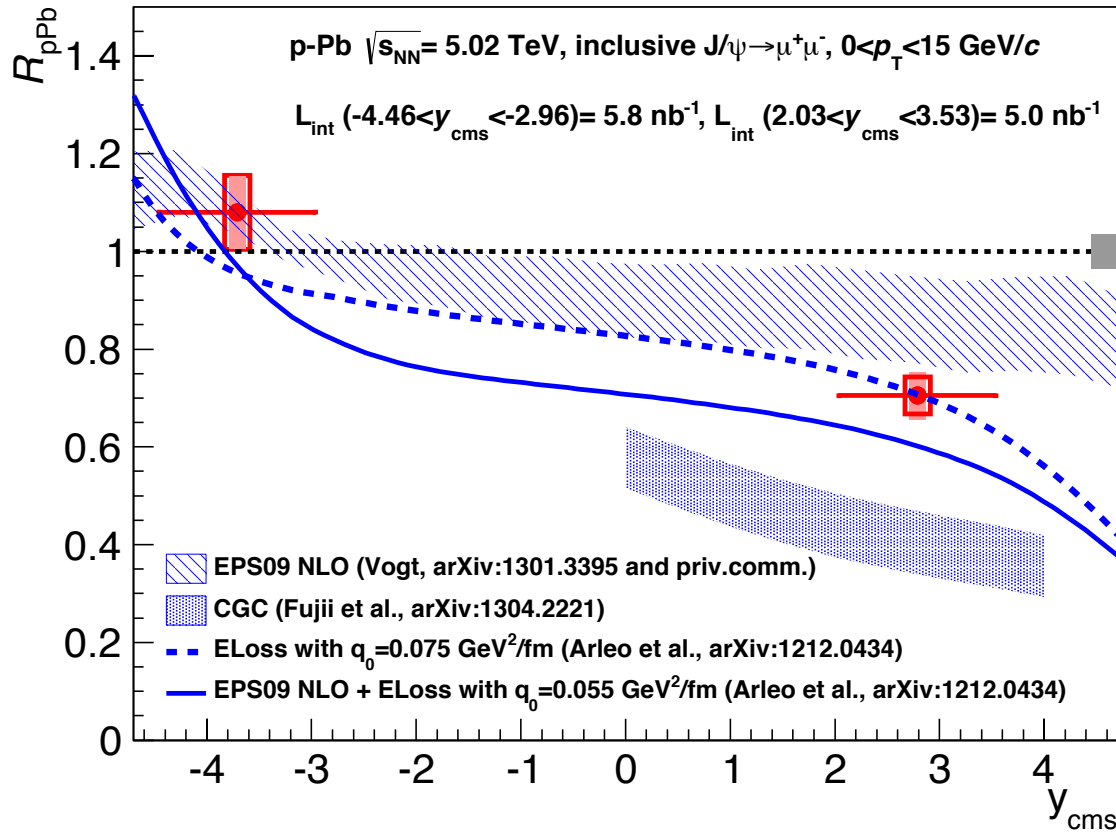
Suppression at forward rapidities

$R_{FB}(y_{cms})$



- No dependence of R_{FB} on rapidity
- Calculations including both shadowing and energy loss seems consistent with data

Integrated R_{pPb}



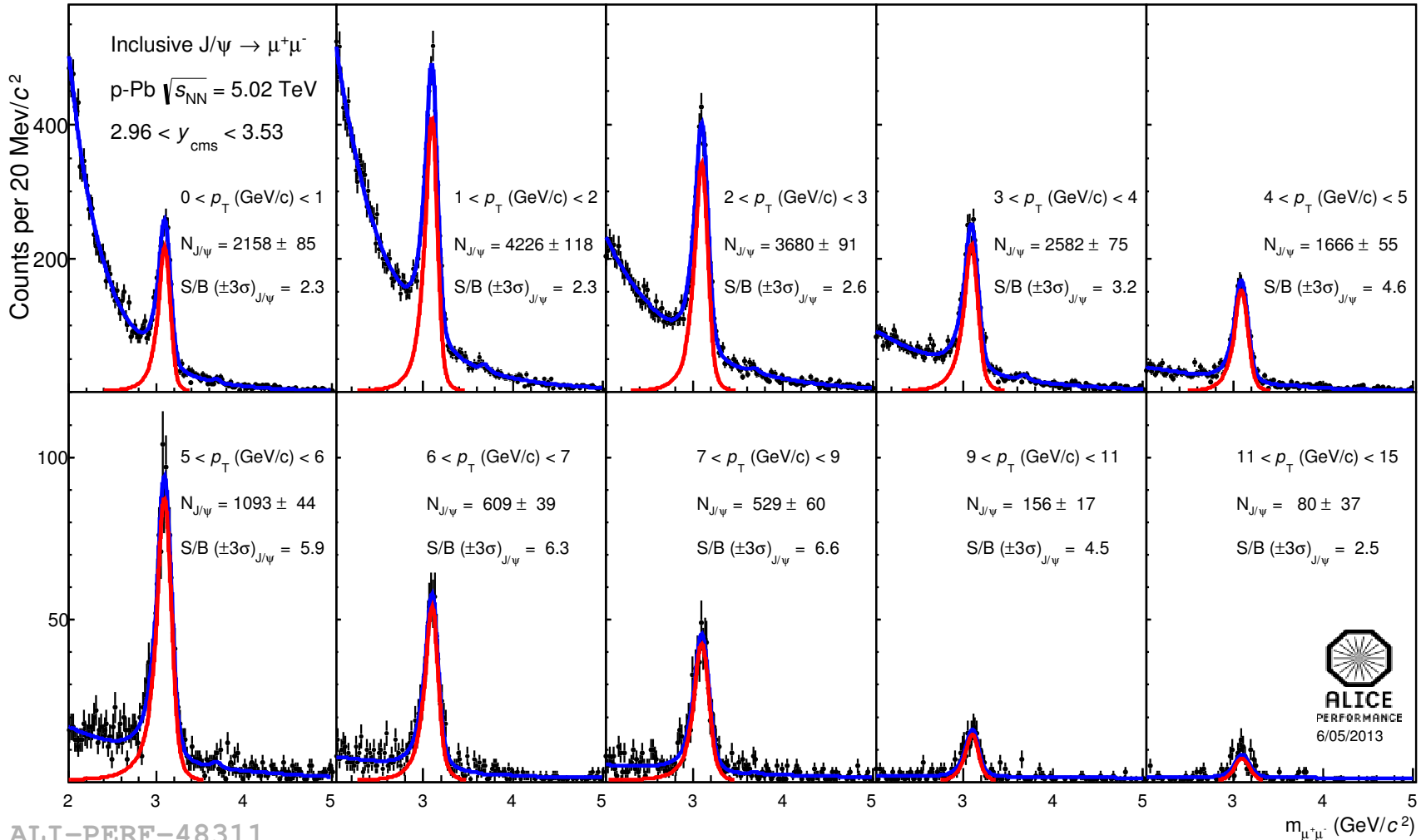
2.03 < y < 3.53

0.70 ± 0.01 (stat.) ± 0.04 (syst.uncorr.) ± 0.03 (syst.part.corr.) ± 0.03 (syst.corr.)

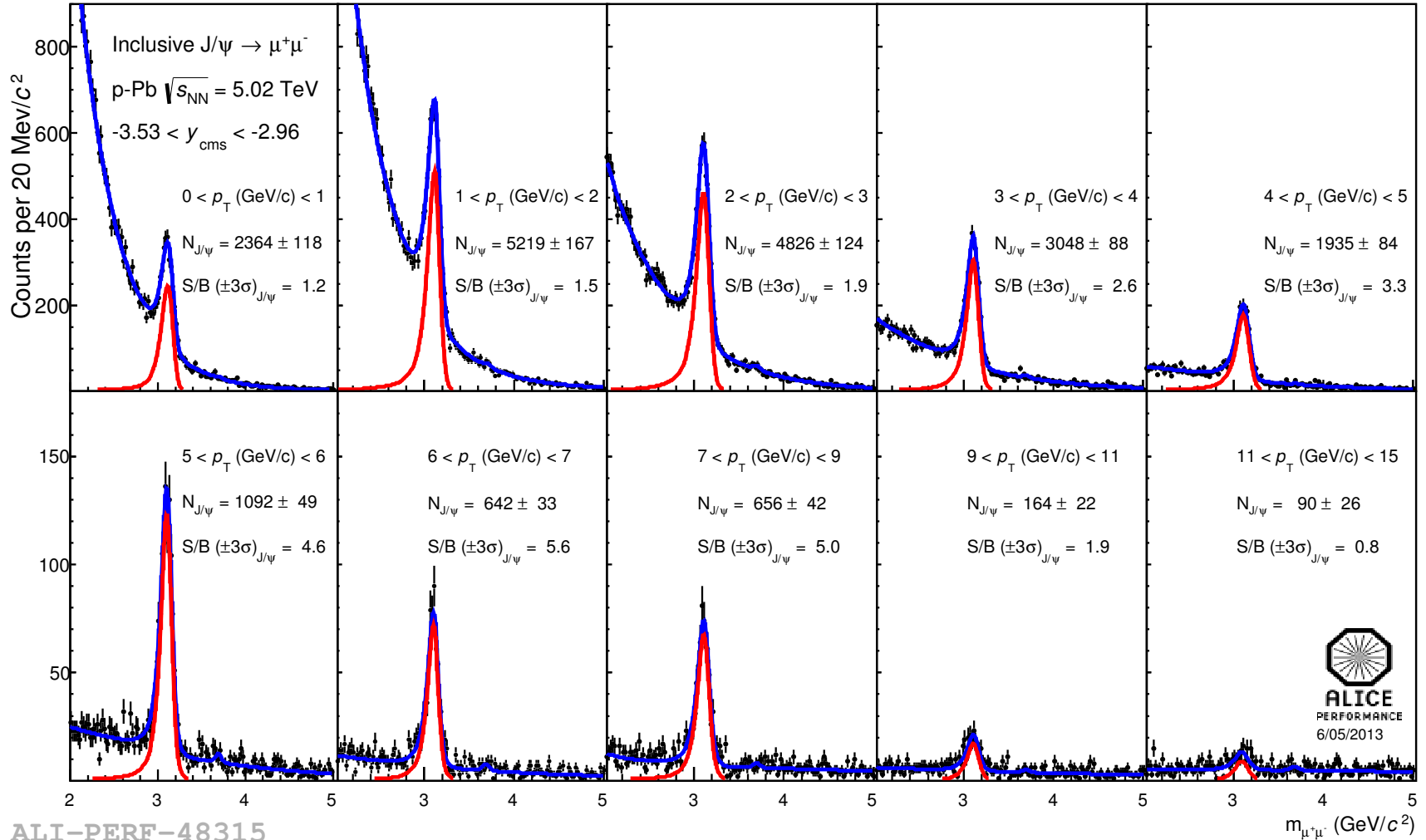
-4.46 < y < -2.96

1.08 ± 0.01 (stat.) ± 0.08 (syst.uncorr.) ± 0.07 (syst.part.corr.) ± 0.04 (syst.corr.)

Signal extraction in different p_T bins (p-Pb)



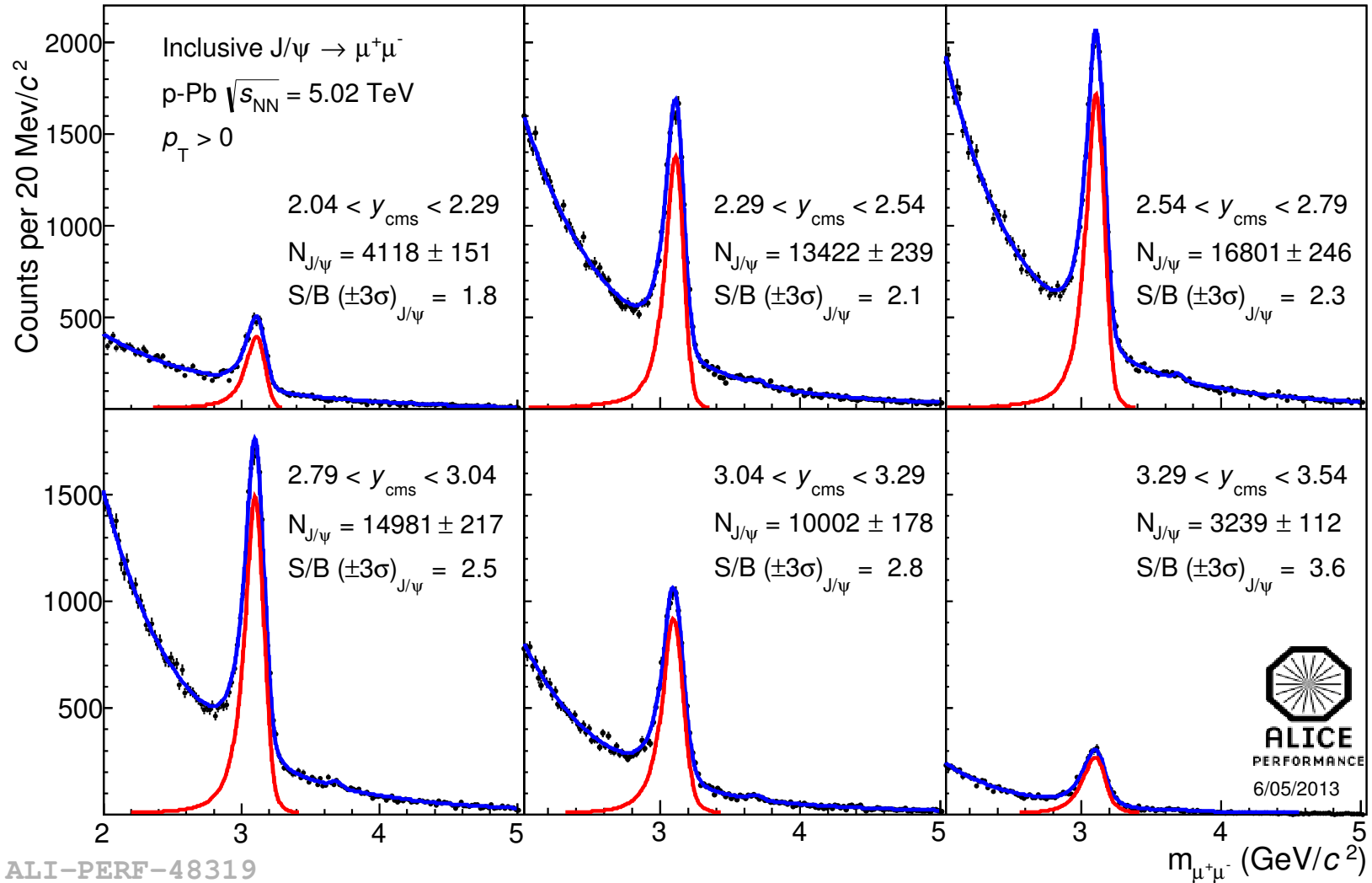
Signal extraction in different p_T bins (Pb-p)



ALI-PERF-48315

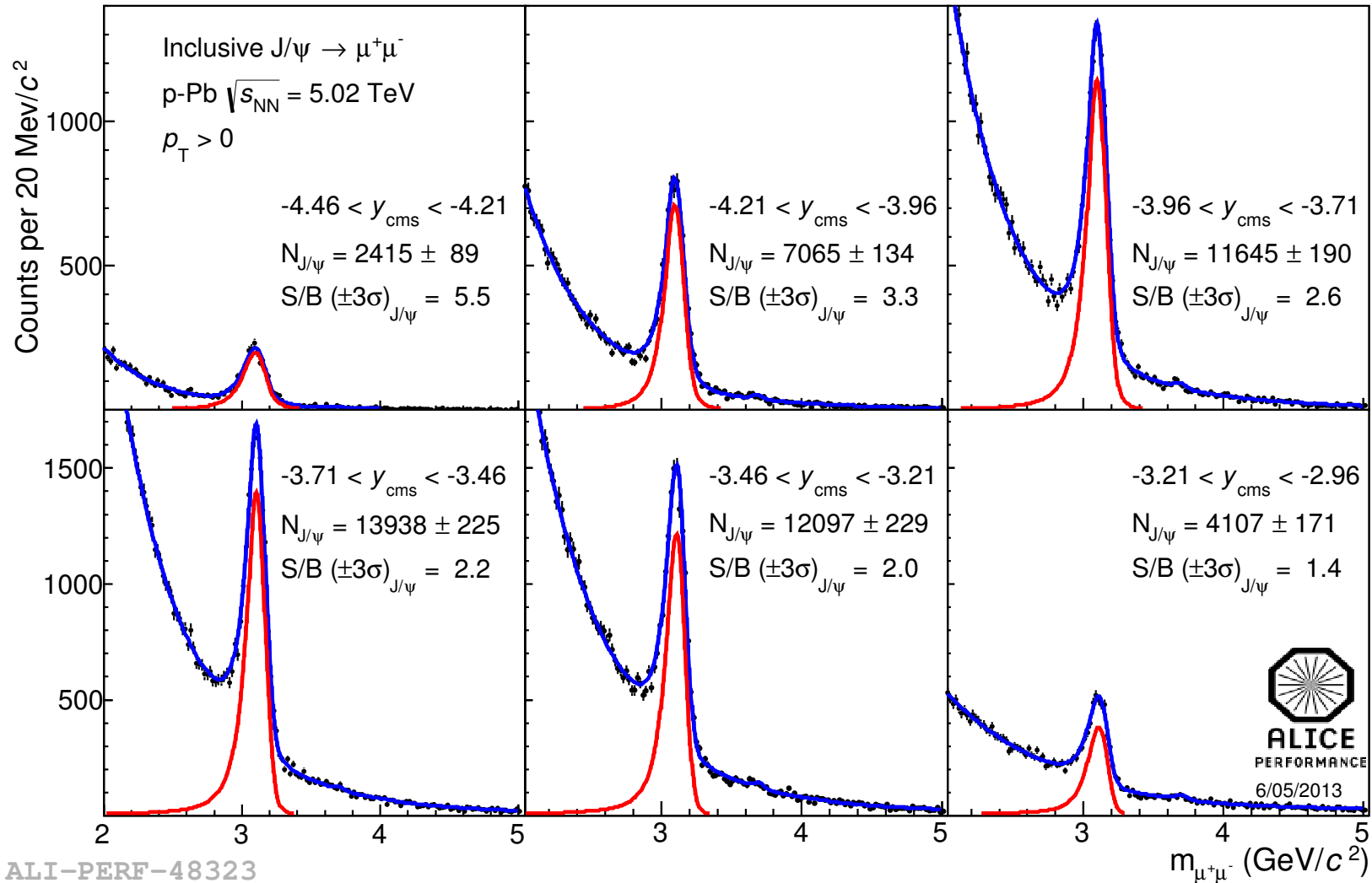


Signal extraction in different y bins (p-Pb)

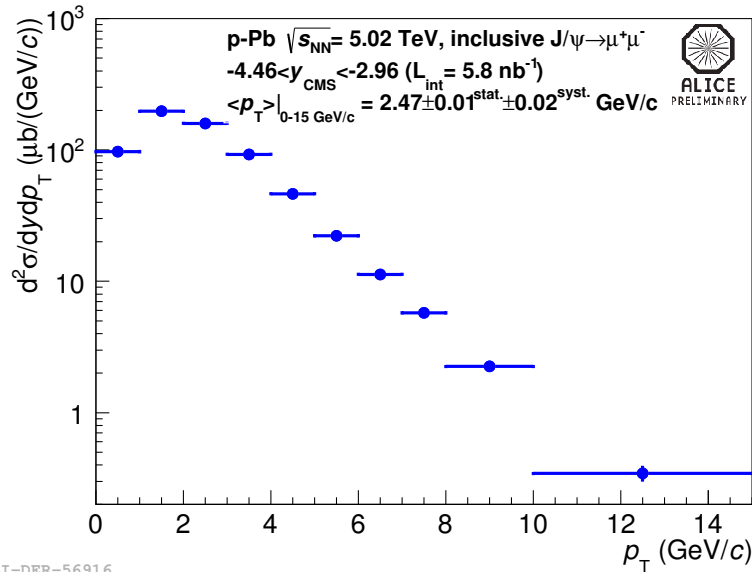


ALI-PERF-48319

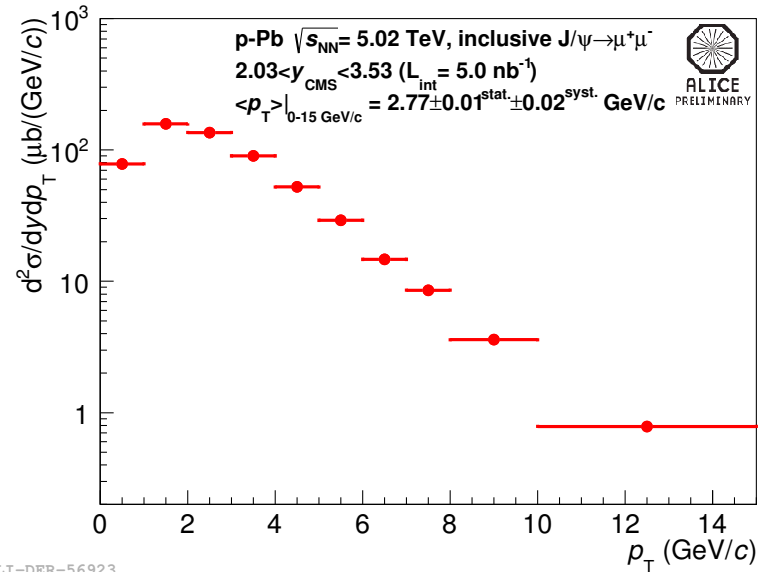
Signal extraction in different y bins (Pb-p)



$d^2\sigma/dydp_T$ with $\langle p_T \rangle$



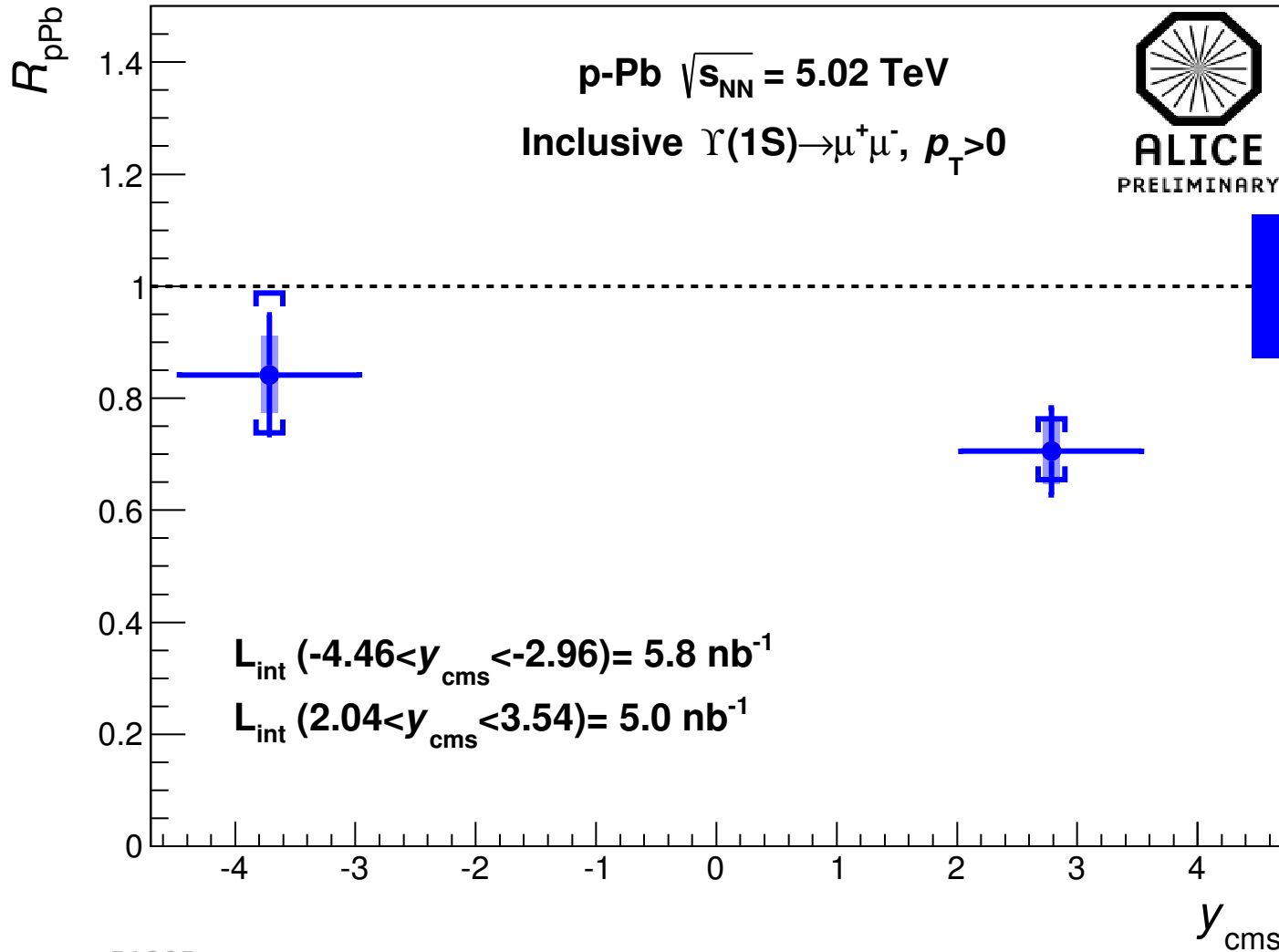
ALI-DER-56916



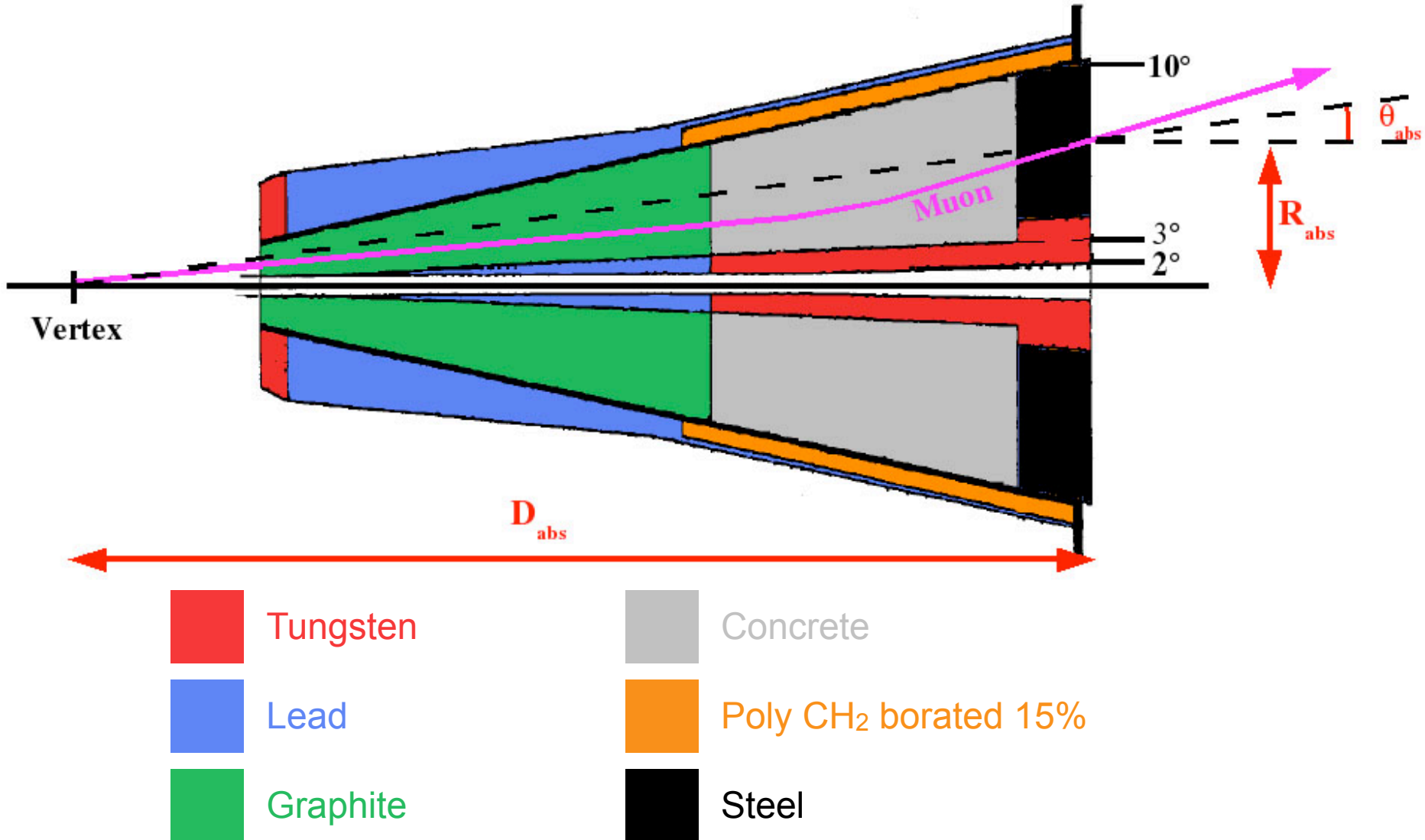
ALI-DER-56923

system (energy)	y_{CMS} -range	$\langle p_T \rangle$	$\langle p_T \rangle$ computation range
pp (2.76 TeV)	2.5 - 4.0	$2.28 \pm 0.07 \pm 0.04$	$0 < p_T < 8 \text{ GeV}/c$
pp (7 TeV)	2.5 - 4.0	$2.44 \pm 0.09 \pm 0.06$	$0 < p_T < 8 \text{ GeV}/c$
Pb-p (5.02 TeV)	-4.46 ; -2.96	$2.47 \pm 0.01 \pm 0.02$	$0 < p_T < 15 \text{ GeV}/c$
Pb-p (5.02 TeV)	-3.53 ; -2.96 (common range)	$2.56 \pm 0.01 \pm 0.02$	$0 < p_T < 15 \text{ GeV}/c$
p-Pb (5.02 TeV)	2.96 ; 3.53 (common range)	$2.71 \pm 0.01 \pm 0.02$	$0 < p_T < 15 \text{ GeV}/c$
p-Pb (5.02 TeV)	2.5 - 4.0	$2.77 \pm 0.01 \pm 0.02$	$0 < p_T < 15 \text{ GeV}/c$

Upsilon R_{pPb}



Muon absorber



Signal shape functions formulas

Extended Crystal Ball

$$f(m) = N \times \begin{cases} \exp\left(-\frac{(m-\bar{m})^2}{2\sigma^2}\right), & \text{for } \frac{(m-\bar{m})}{\sigma} > -\alpha \\ A \left(B - \frac{m-\bar{m}}{\sigma}\right)^{-n}, & \text{for } \frac{(m-\bar{m})}{\sigma} \leq -\alpha \\ C \left(D + \frac{m-\bar{m}}{\sigma}\right)^{-n'}, & \text{for } \frac{(m-\bar{m})}{\sigma} \geq -\alpha' \end{cases}$$

$$\begin{aligned} A &= \left(\frac{n}{|\alpha|}\right)^n \exp\left(-\frac{|\alpha|^2}{2}\right) \\ B &= \frac{n}{|\alpha|} - |\alpha| \\ C &= \left(\frac{n'}{|\alpha'|}\right)^{n'} \exp\left(-\frac{|\alpha'|^2}{2}\right) \\ D &= \frac{n'}{|\alpha'|} - |\alpha'| \end{aligned}$$

NA60 function

$$f(m) = N \times \exp\left(-\frac{(m-\bar{m})^2}{2\sigma_{NA60}^2}\right)$$

$$\sigma_{NA60} = \begin{cases} \sigma \left(1 + p_1(m_1 - m)^{p_2 - p_3 \sqrt{m_1 - m}}\right), & \text{for } m < m_1 \\ \sigma, & \text{for } m_1 \leq m < m_2 \\ \sigma \left(1 + p_4(m - m_2)^{p_5 - p_6 \sqrt{m - m_2}}\right), & \text{for } m \geq m_2 \end{cases}$$

N, σ (J/Ψ width), m (J/Ψ mass) are left free when fitting the data
all other parameters are fixed on tuned MC

Interpolation : preliminary vs paper

Preliminary results (based on a different interpolation method)

$$BR \times \sigma_{pp}^{J/\psi} (2.03 < y_{cms} < 3.53) = 346_{-48(syst.)}^{+61(syst.)} \text{ nb}$$

$$BR \times \sigma_{pp}^{J/\psi} (-4.46 < y_{cms} < -2.96) = 238_{-40(syst.)}^{+60(syst.)} \text{ nb}$$

Paper results (this talk)

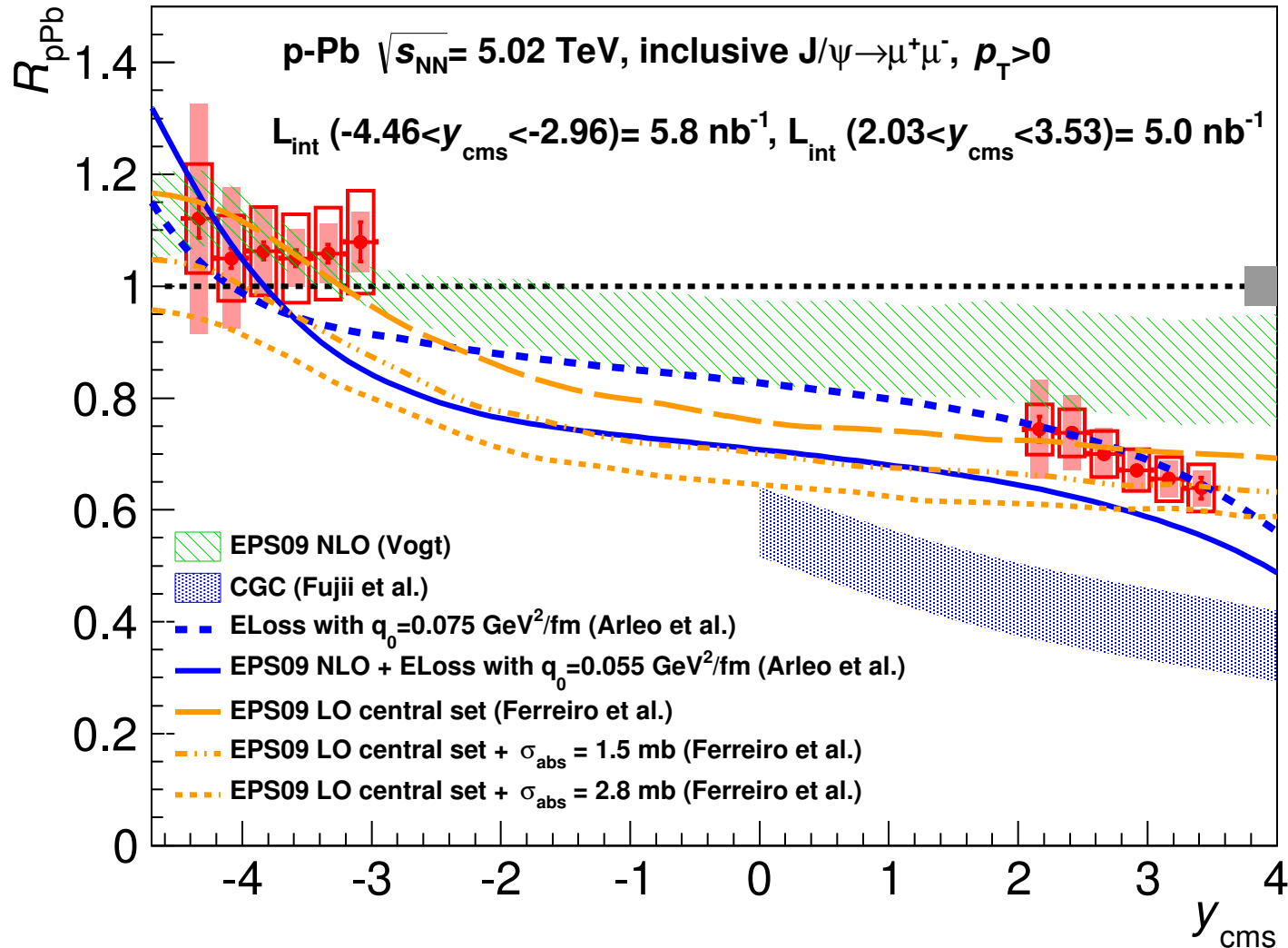
$$BR \times \sigma_{pp}^{J/\psi} (2.03 < y_{cms} < 3.53) = 366 \pm 24 \text{ nb}$$

$$BR \times \sigma_{pp}^{J/\psi} (-4.46 < y_{cms} < -2.96) = 255 \pm 16 \text{ nb}$$

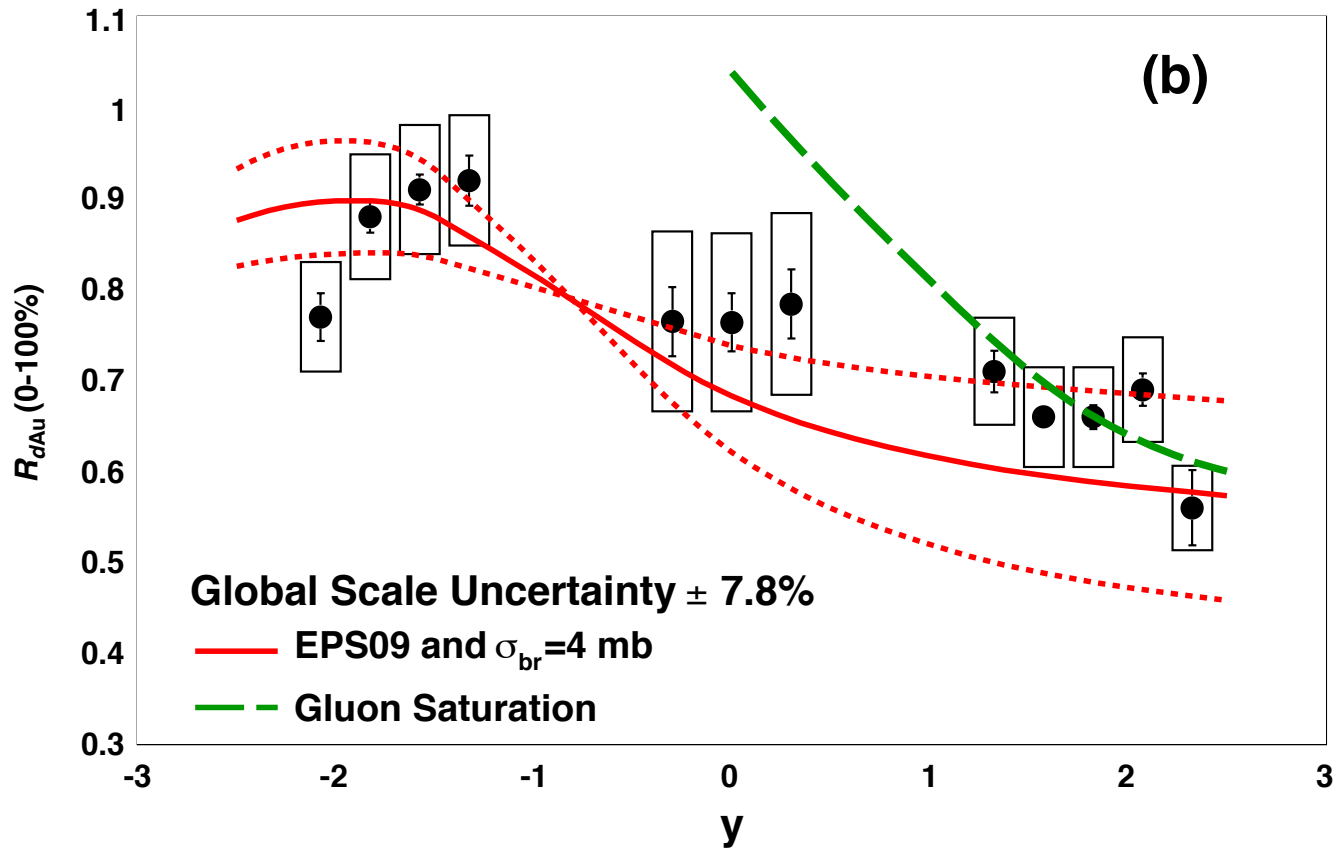
+7%

+5.5%

J/ψ R_{pPb} and R_{PbP} in y bins compared to models

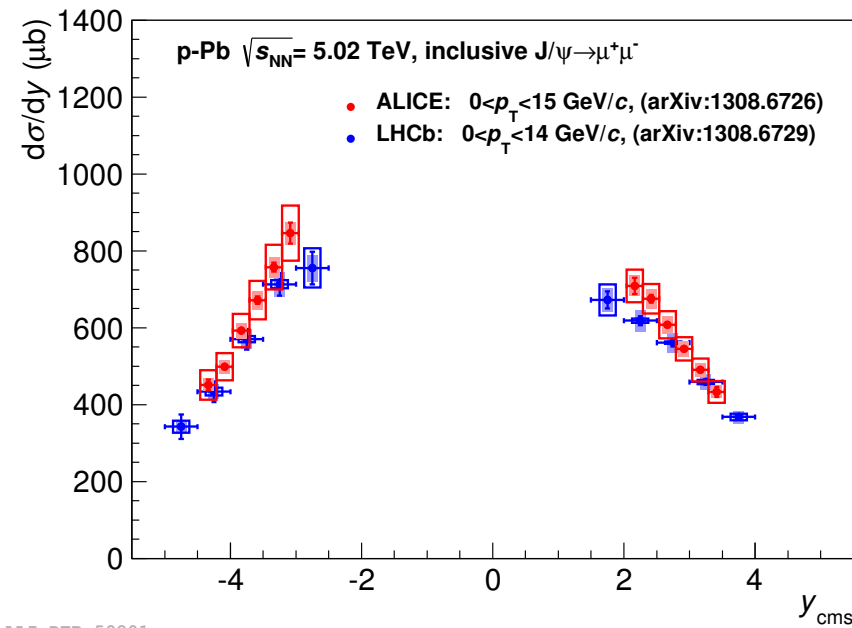


PHENIX data

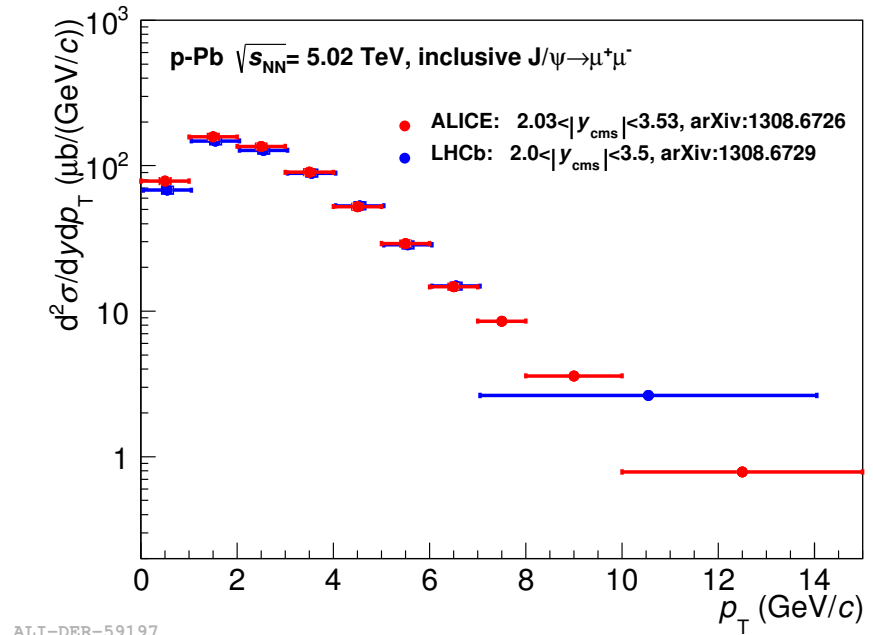


From PRL **107**, 142301 (2011) (Fig.1)

ALICE vs LHCb : cross-sections

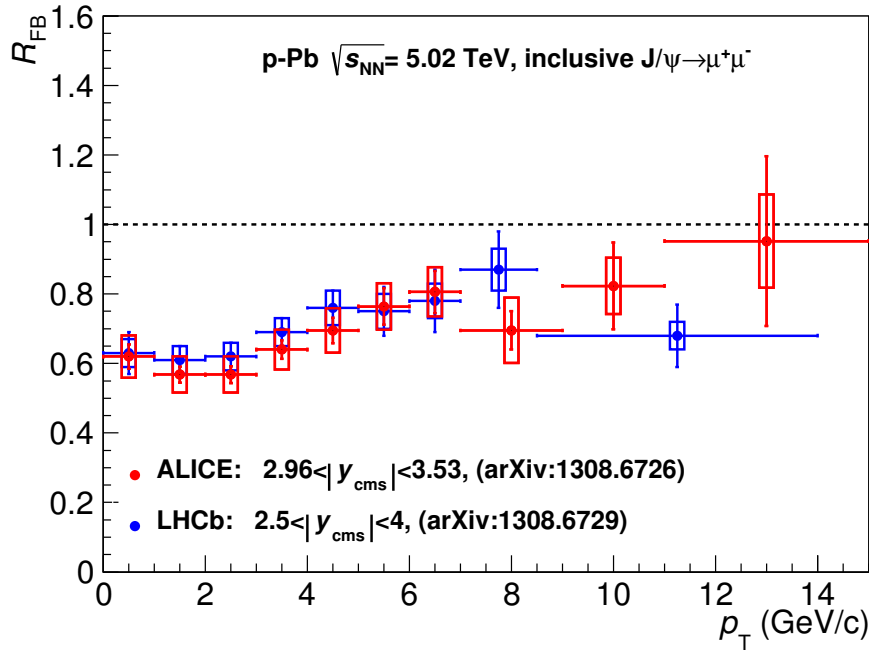


ALI-DER-59201

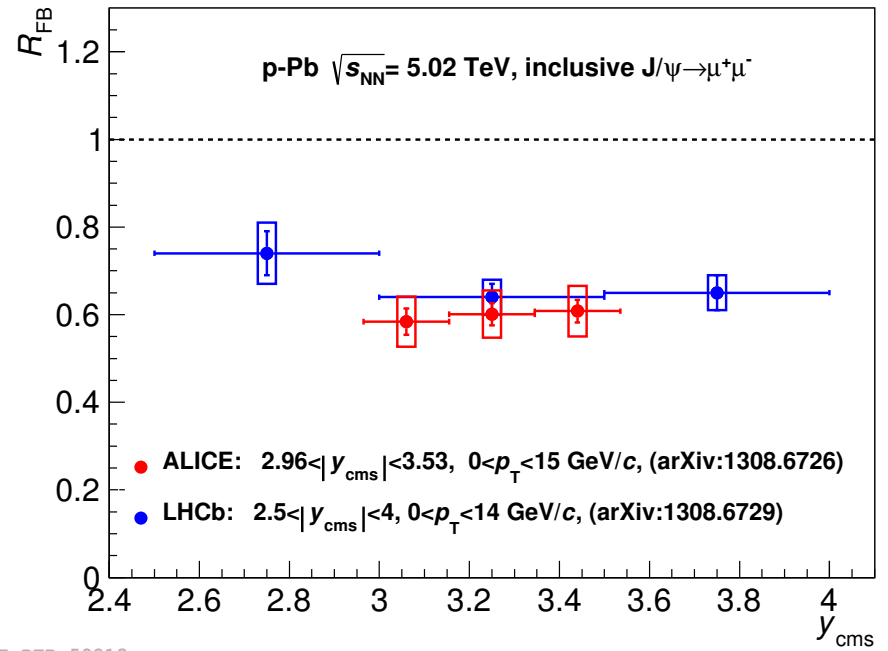


ALI-DER-59197

ALICE vs LHCb : R_{FB}

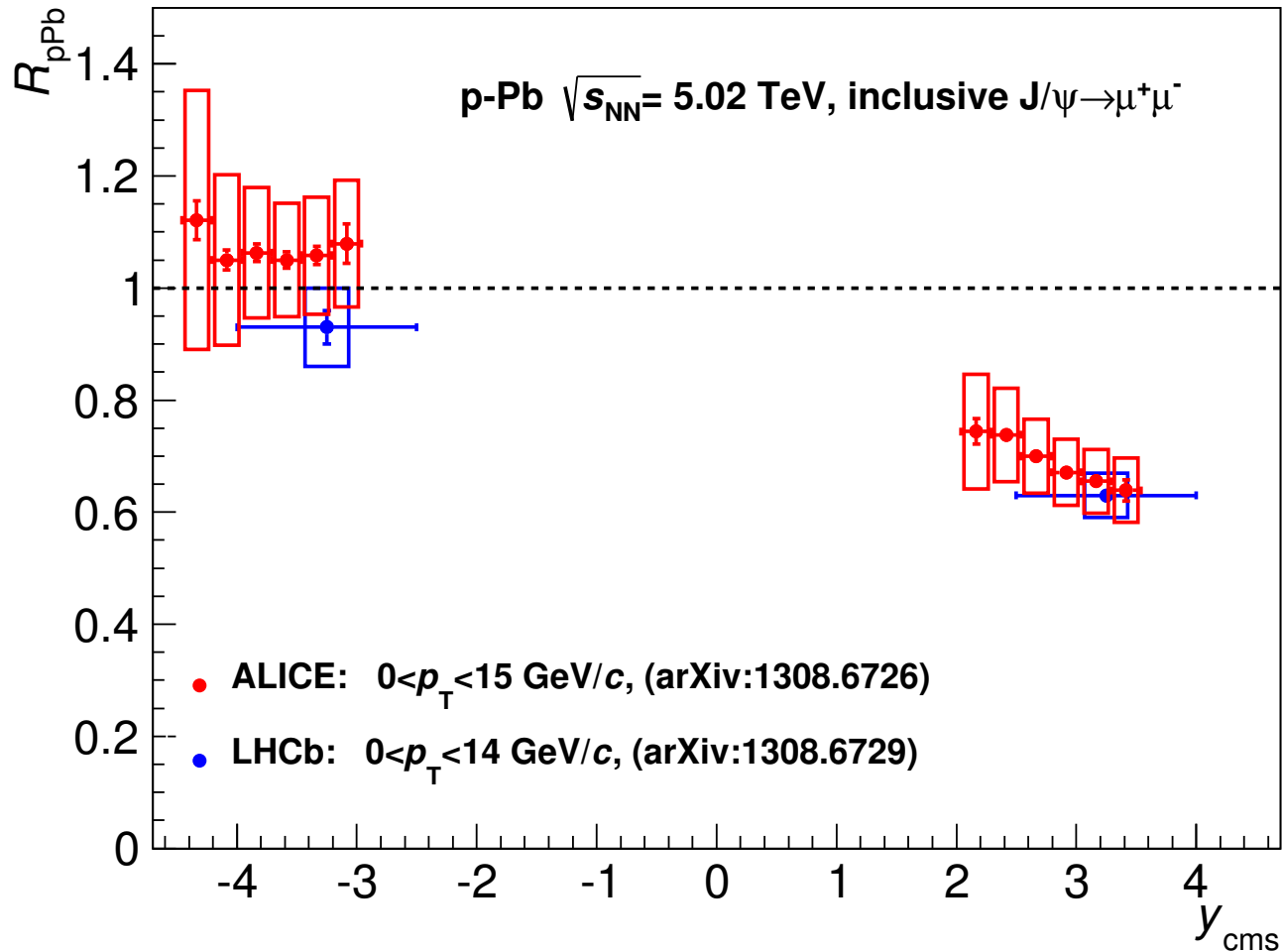


ALI-DER-59217



ALI-DER-59213

ALICE vs LHCb : R_{pPb}



ALI-DER-59209